Assessing the Limitations of Self-Interaction-Corrected Functionals for Describing the Hydrated Electron

Wilberth A. Narvaez,*,† David M. Bartels,‡ and Ward H. Thompson*,†

†*Department of Chemistry, University of Kansas, Lawrence, Kansas, 66045, United States*
‡*Radiation Laboratory, University of Notre Dame, Notre Dame, Indiana 46556, United States*

E-mail: w696n850@ku.edu; wthompson@ku.edu

Abstract

Simulating the hydrated electron using density functional theory is challenging due to the prevalence of self-interaction error in standard functionals. Hybrid functionals like PBEh(40) can reasonably describe the chemistry of an excess electron in water and partially mitigate self-interaction error by incorporating exact Hartree–Fock exchange, but they are computationally expensive making them impractical for large-scale and long-time *ab initio* molecular dynamics simulations. Explicit self-interaction correction schemes that are applied on an orbital-by-orbital basis offer a potential alternative when the correction is limited to the singly-occupied molecular orbital obtained with a generalized gradient approximation functional. Here, we examine whether the Perdew–Zunger self-interaction correction scheme applied to the revPBE functional can provide a computationally efficient and physically sensible alternative to PBEh(40) for the hydrated electron. We find that functionals incorporating a self-interaction correction scheme should be viewed with caution when applied to the hydrated electron and its reactivity. Moreover, we show that it is critical to consider extensive sampling and diverse chemical environments when validating their performance.

Introduction

Hydrated electrons, e^-_{aq}, are ubiquitous species in the radiation chemistry of aqueous solutions and are among the most powerful reducing agents available for advanced reduction processes.[1–6] Structurally, they are excess electrons not bound to any individual atom or molecule but are instead localized within a cavity in the solvent structure.[7,8] The extremely negative reduction potential of e^-_{aq}, $E^\circ \approx -2.9$ V, drives its facile reactivity with many organic and ionic species across a wide range of conditions. Since the early 1960s, numerous independent experiments have examined these reactions and generated a wealth of thermodynamic and kinetic data.[9–17] However, a detailed mechanistic understanding of these one-electron

transfer reactions remains elusive.

The intrinsically quantum mechanical nature of the hydrated electron has challenged theoretical modeling. Nevertheless, significant insight augmenting experimental measurements has been obtained over the past two decades from computer simulations. While one-electron pseudopotentials have been, and continue to be, a valuable approach within molecular dynamics (MD) simulations,[18,19] density functional theory (DFT) has more recently emerged as a key computational technique,[20–23] especially with respect to reactivity.[24–28] However, the cavity-bound structure is not the only possible one for the hydrated electron. It can also delocalize (which is a higher energy state) or react with water (a process that determines its $< 300\mu$s lifetime[3,14] in neat water) and DFT functionals can struggle to accurately describe the relative energies (and barriers) for these outcomes.[29]

These difficulties are particularly challenging to overcome with generalized gradient approximation (GGA) functionals, which suffer from self-interaction error (SIE) arising from the unphysical interaction of an electron with its own charge density. Thus, to describe the electronic levels of an excess electron in neat water at room temperature, DFT is commonly employed with the hybrid PBEh(40) functional, as proposed by Pasquarello *et al.*[22,30] using 100% PBE correlation, 60% PBE exchange, and 40% exact Hartree–Fock exchange. Unfortunately, despite the successes of this functional in describing the chemistry of the hydrated electron,[6] the inclusion of the four-center Hartree–Fock exchange integrals severely limits the system sizes and simulation times that are computationally accessible with it.

An alternative to the computationally expensive addition of exact Hartree–Fock exchange is a direct self-interaction correction (SIC) scheme that works *via* the explicit subtraction of the Hartree (H) and exchange–correlation (XC) self-interaction energy on an orbital-by-orbital basis.[31–33] As these explicit SIC schemes are commonly applied only on the singly occupied molecular orbital of a doublet-multiplicity system computed using a GGA functional, they offer a potentially efficient alternative to PBEh(40) for the hydrated electron. Notably, modified versions of the Perdew–Zunger (PZ) SIC approximation have already been employed with the BLYP and PBE functionals to simulate the dynamics and reactivity of the hydrated electron,[25,26,34] but a systematic investigation of their behavior is lacking.

The computationally demanding evaluation of the orbital-dependent PZ-SIC energies can be greatly reduced by the use of the restricted open-shell formalism, in which the self-interaction correction is applied only to the spin density associated with the singly occupied molecular orbital. This avoids the computational bottlenecks and technical difficulties associated with the treatment of hundreds of molecular orbitals in the liquid phase. In this particular formulation, the correction is effectively expressed as a scaled Hartree and exchange–correlation energy functional of the spin density, $m = \rho_\alpha - \rho_\beta$, where ρ_α and ρ_β are the spin-up and spin-down electron densities, respectively.[33] The resulting self-interaction-corrected energy is

$$E_{\mathrm{SIC}} = E_{\mathrm{KS}}[\rho_\alpha, \rho_\beta] - \Delta E_{\mathrm{SIC}}[\rho_\alpha, \rho_\beta], \quad (1)$$

where

$$\Delta E_{\mathrm{SIC}} = c_{\mathrm{H}} E_{\mathrm{H}}[m] + c_{\mathrm{XC}} E_{\mathrm{XC}}[m, 0]. \quad (2)$$

The scaling variables c_{H} and c_{XC} are empirically tunable parameters that can, in principle, be optimized for any GGA func-

tional to approximately reproduce physical observables predicted by higher levels of theory.[33] In this work, the spin density obtained with the PBEh(40)-D3 functional is chosen as the optimization target, as it provides a qualitatively sensible description of the hydrated electron by partially mitigating the self-interaction error present in the PBE functional through the inclusion of exact Hartree–Fock exchange.[22]

In this Paper, we present a systematic investigation of the PZ-SIC approximation applied to the revPBE-D3 description of the hydrated electron in water. We select revPBE as the underlying functional to be optimized due to its better description of the structure and dynamics of liquid water[35,36] compared to PBEh(40). Importantly, we examine not only the predictions of different SIC models for the hydrated electron in different water configurations, but also their performance in simulating the equilibrium dynamics of the hydrated electron and its reactivity with Zn(II). We show that the latter two tests are critical to determining the quality of an SIC description.

Computational Methods

We start by propagating a 2 ns classical MD trajectory for a water simulation box containing one chloride ion using the Large-Scale Atomic/Molecular Massively Parallel Simulator (LAMMPS) code.[37] From the last 240 ps of these dynamics we extract configurations every 20 ps, which are used to initialize twelve independent 2 ps DFT molecular dynamics trajectories. Finally, 10 ps hydrated electron DFT-MD trajectories are initiated by removing the chlorine atom from the final configuration of each of the aqueous Cl^- DFT simulations and changing the system's spin multiplicity to a doublet state. Both the aqueous Cl^- and e^-_{aq} DFT simulations are carried out with the QUICKSTEP module within the CP2K quantum chemistry suite.[38]

All hydrated electron trajectories are propagated under periodic boundary conditions and using the canonical (NVT) ensemble with a temperature of 25°C and a density of 0.997 g/cm^3 with 64 water molecules. Simulations involving the Zn(II) ion include 128 water molecules at a total solution density of 1.0024 g/cm^3. Trajectories meant to simulate the thermalization of an excess electron injected into neat water used a simulation cell with a side length of 9.81 Å and 32 waters. Classical trajectories used a 1 fs time step to propagate the dynamics of a simulation cell containing dozens of SPC/Fw waters[39] and one chloride ion modeled as a Lenard–Jones sphere with charge $-e$, $\epsilon = 0.1148$ kcal/mol, and $\sigma = 5.029$ Å. The classical Zn(II) ion was modeled with charge $+2e$, $\epsilon = 0.25$ kcal/mol, and $\sigma = 1.95$ Å. DFT trajectories are propagated with a 0.5 fs time step and a 10^{-5} a.u. SCF convergence threshold, using a TZVP valence-electron basis set in combination with the Goedecker–Teter–Hutter pseudopotentials for the core-electrons. Grimme's D3 dispersion empirical correction[40] is used to improve the modeling of long-range dispersion forces of all DFT descriptions.

For the hybrid PBEh(40)-D3 molecular dynamics simulations, we employ the unrestricted Kohn–Sham formalism with a plane-wave cutoff of 600 Ry. To accelerate the calculation of the Hartree–Fock integrals, we use the auxiliary density matrix method with the cFIT3 auxiliary basis set.[41] On the other hand, we found it necessary, to accurately capture the fine details of the numerical spin density, to use a plane-wave cutoff of 1000 Ry for the revPBE-D3 and SIC-revPBE-D3 restricted open-shell Kohn-Sham (ROKS) simulations. All DFT simu-

lations use 4 multigrids with a grid-mapping cutoff of 60 Ry. As shown in Fig. S1, our cutoffs are chosen to predict well-converged energies and forces.

Results

Self-Interaction-Corrected revPBE-D3 Spin-Density Optimization

We first assess the performance of the PZ-SIC approximation in predicting the radius of gyration, R_g, of the spin density for hydrated electron configurations generated using the PBEh(40) functional. Specifically, configurations are extracted every 125 fs from a 10 ps PBEh(40)-D3 hydrated electron simulation with 64 water molecules at 25°C and 0.997 g/cm^3. The corresponding spin density for each extracted configuration is recalculated using SIC-modified revPBE-D3 functionals, constructed by systematically varying the contributions of E_{H} and E_{XC} in Eq. (2). The results of these calculations are presented in Fig. 1, where the SIC-revPBE-D3 R_g are compared to that for the original PBEh(40)-D3 functional (recalculated with a 1000 Ry plane-wave cutoff to provide a direct comparison).

The results shown in Fig. 1 for the revPBE-D3 functional with no SIC show that it overdelocalizes the spin density, even when evaluated for configurations extracted from a PBEh(40) trajectory with a well-equilibrated solvent cavity for the hydrated electron. Inclusion of the Hartree self-interaction correction in the functional confines the spin density to the solvent cavity, as evidenced by the smaller radius of gyration for the SIC-revPBE-D3 functionals with E_{H} scaled by $c_{\mathrm{H}} = 0.15$, $c_{\mathrm{H}} = 0.20$, and $c_{\mathrm{H}} = 0.30$. These SIC-modified functionals will hereafter be designated as SIC(15,0), SIC(20,0) and SIC(30,0), respectively, and

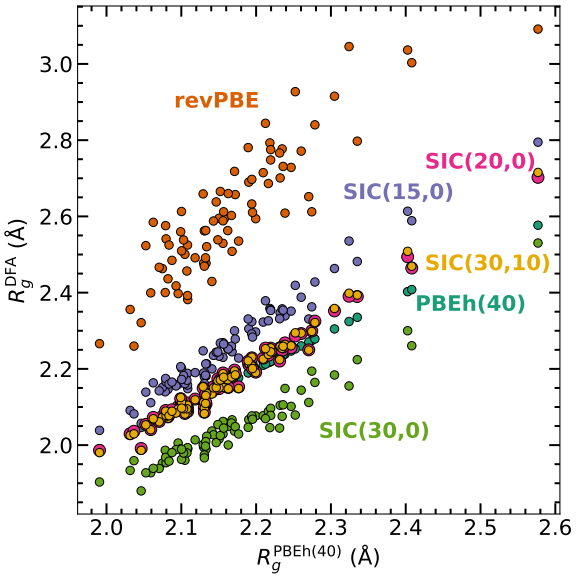

Figure 1: Correlation between the radius of gyration, R_g, of the spin density obtained with revPBE-D3 (orange), SIC(15,0)-revPBE-D3 (purple), SIC(20,0)-revPBE-D3 (pink), SIC(30,0)-revPBE-D3 (green), and SIC(30,10)-revPBE-D3 (yellow), and that obtained with PBEh(40)-D3 (cyan). All configurations originate from a single PBEh(40)-D3 hydrated electron simulation with 64 waters at 25°C and 0.997 g/cm^3.

this SIC($c_{\mathrm{H}} \times 100$,$c_{\mathrm{XC}} \times 100$) naming convention is adopted for all SIC-revPBE-D3 functionals in Fig. 1 and throughout the manuscript. (Additional results for SIC(15,5), SIC(20,5), and SIC(30,5) functionals are shown in Fig. S2.)

In general, the degree of localization of the excess electron increases upon addition of the Hartree term, E_{H} in Eq. (2), but decreases with increasing contributions from the exchange–correlation term, E_{XC}. Namely, SIC(15,0) significantly ameliorates the overdelocalization of the revPBE-D3 description. The SIC variant with a 20% E_{H} correction on the spin density gives R_g values in very good agreement with the PBEh(40)-D3 results, suggesting it may

be an accurate SIC-based description for the hydrated electron. Further scaling the Hartree term by using the SIC(30,0) functional predicts a hydrated electron that is too localized. However, inclusion of exchange–correlation in the self-interaction correction scheme, in the SIC(30,10) functional, increases the spatial extent of the spin density, resulting in better agreement, compared to SIC(30,0), with the radii of gyration given by the reference PBEh(40)-D3 functional. Indeed, the SIC(30,10) and SIC(20,0) functionals predict R_g values that agree well both with each other and the PBEh(40)-D3 results.

Hydrated Electron Dynamics with Self-Interaction-Corrected Functionals

It is important to recognize that reproduction of the spin density for configurations obtained from an MD simulation with PBEh(40)-D3 does not guarantee stable hydrated electron dynamics with the SIC description. Accordingly, all functionals presented in Fig. 1 were also used to propagate ensembles of 12 independent 10 ps DFT-MD trajectories initiated with configurations uninfluenced by the PBEh(40)-D3 functional, specifically, from equilibrated revPBE-D3 simulations of a Cl^- ion in aqueous solution (from which the chlorine atom is removed to generate a hydrated electron, as described in Sec. 2.

The average radius of gyration of the spin density obtained over the course of these simulations is shown in Fig. 2a for the different functionals. As expected, revPBE-D3 fails to yield a stable hydrated electron. Even when a solvent cavity of the appropriate size is present at the start of the simulation (by initiating from a solvated Cl^- ion configuration with the Cl atom removed),

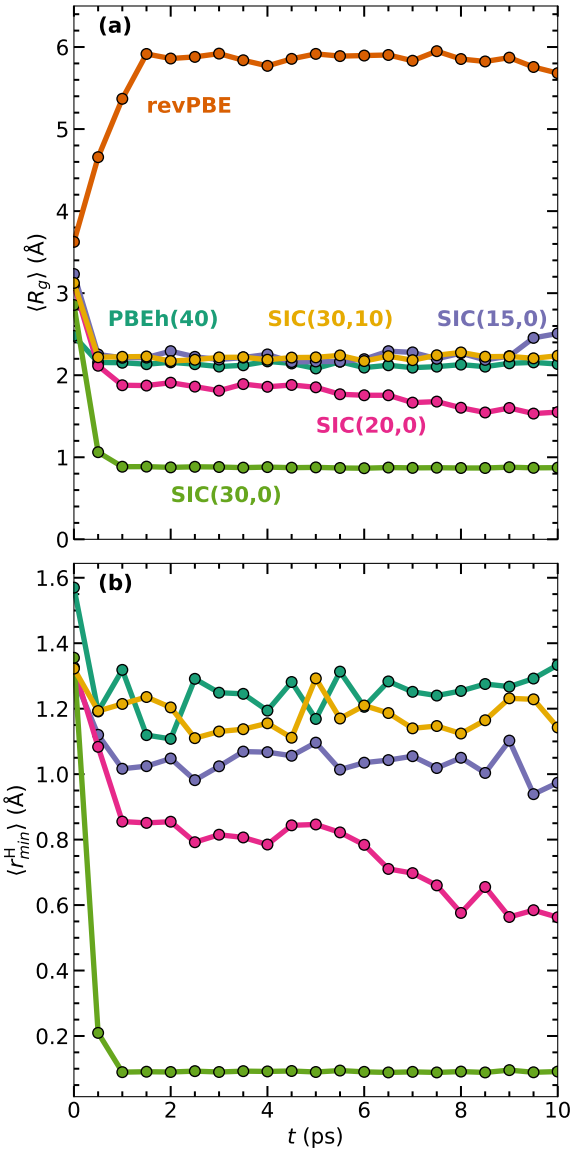

Figure 2: **a.** Average radius of gyration for the spin density obtained with PBEh(40)-D3, revPBE-D3, and SIC-revPBE-D3 functionals. **b.** Distance between the spin density centroid and the nearest hydrogen atom. Averages are computed over 12 independent trajectories per functional, and the same set of initial configurations is used to initiate corresponding trajectories across all revPBE variants.

the excess electron delocalizes throughout the simulation cell in less than 1 ps. At the opposite extreme, the SIC(30,0) trajec-

tories result in reaction of the excess electron with a water molecule to generate H· within a few hundred fs after initiation of the simulation, a reaction that is known experimentally to occur on a timescale longer than μs.[3,14] This is reflected in the average distance between the spin density's centroid and the nearest hydrogen atom, shown in Fig. 2b and Fig. S3. This overlocalization (which results here in a lowering of the barrier to reaction with water) is a well-known failure of the SIC scheme and arises from an overcorrection of the Hartree energy.

The other three SIC functionals give intermediate values of the average radius of gyration. Interestingly, while the SIC(15,0) functional predicts an $\langle R_g \rangle$ that is too large for PBEh(40) configurations, Fig. 1, when used to propagate a DFT-MD trajectory, it predicts an average radius of gyration of $\sim$ 2.3 Å. This reasonably reproduces the average PBEh(40) R_g of 2.1 Å and is in good agreement with the experimental value of 2.45 Å inferred from moment analysis of the absorption spectrum.[42] The nearest-neighbor distance of $\langle r^{\mathrm{H}}_{min} \rangle \sim 1$ Å is also in reasonable agreement with the e^-_{aq}–H radial distribution function typically observed for cavity-like hydrated electrons.

In contrast, while the radius of gyration obtained using SIC(20,0) to recalculate the spin density of PBEh(40)-D3 configurations is in excellent agreement with the results of the hybrid (Fig. 1), the 1.8 Å average radius of gyration it predicts when used to propagate dynamics agrees neither with PBEh(40)-D3 nor experiment. In addition, the average distance between the electron and the nearest H atom lies below 1 Å and decreases with time, inconsistent with a stable cavity structure. Inspection of the individual trajectories reveals an even more complex story. The behavior can be visualized through a combination of the electron–water radial distribution functions (RDFs), presented in Fig. 3 and the probability density functions of R_g and r^{H}_{min} estimated with Gaussian kernels, shown in Fig. 4.

Despite the reasonable $\langle R_g \rangle$ value from the DFT-MD simulations, one of the twelve SIC(15,0) trajectories results in the excess electron localizing on a hydrogen atom, *e.g.*, reacting with a water molecule, as shown in Fig. S5. This can be seen in the peak around $R_g \simeq 1$ Å and $r^{\mathrm{H}}_{min} \simeq 0$ in the probability distributions in Fig. 4 indicative of formation of H·. As observed for all SIC(30,0) trajectories, this unphysical localization occurs at the start of the simulation and must arise from an overcorrection of the self-interaction error. The inspection also identified an SIC(15,0) trajectory in which the excess electron became delocalized after more than 9 ps of simulation time, suggesting that attempts to eliminate overlocalization by further decreasing the value of c_{H} alone would be futile. The smaller average R_g for the SIC(20,0) ensemble is representative of a greater number of overlocalized/reactive trajectories. This can be seen in the R_g and r^{H}_{min} distributions in Fig. 4, where the peaks at $R_g \simeq 1$ Å and $r^{\mathrm{H}}_{min} \simeq 0$ are even larger in amplitude than for the SIC(15,0) case. This behavior highlights a major limitation of the present self-interaction correction scheme as it is commonly implemented: it is not possible to adequately compensate for the self-interaction error of a GGA functional by exclusively remedying the Hartree energy of the singly occupied molecular orbital.

In contrast to the SIC(15,0) and SIC(20,0) functionals, the excess electron–water radial distribution function of the SIC(30,10) functional exhibits excellent agreement with the PBEh(40)-D3 data, as presented in Fig. 3. Furthermore, Fig. 4a shows that inclusion of both the Hartree and exchange-correlation correction terms yields a radius of gyration in good agreement with exper-

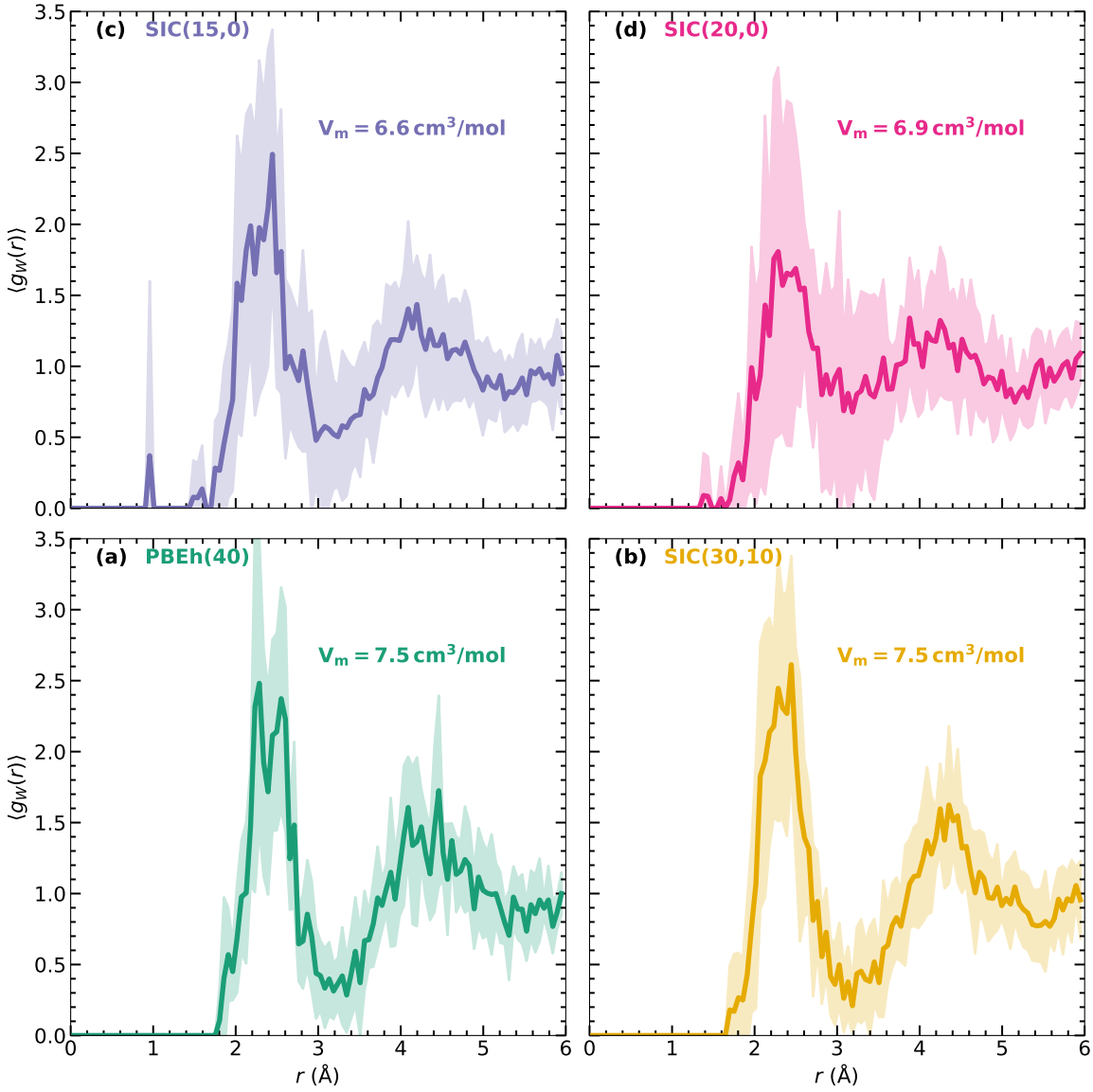

Figure 3: Excess electron–water radial distribution functions are computed using the centroid of the spin density and the center-of-mass of the water molecules, and averaged over 12 independent trajectories per functional. Shaded error envelopes denote one standard deviation. Purple, pink, yellow, and cyan curves correspond to SIC(15,0)-revPBE-D3, SIC(20,0)-revPBE-D3, SIC(30,10)-revPBE-D3, and PBEh(40)-D3, respectively.

iment, as the values are confined mostly to the 2.0–2.6 Å region. Furthermore, Figs. 4b and S5 show that the early time overlocalization of the excess electron, observed for the SIC(30,0) functional, is suppressed in the SIC(30,10) case by inclusion of the exchange–correlation correction, without compromising the stability of the hydrated electron.

While the SIC(30,10) functional provides a more accurate description of the hydrated electron than its SIC(15,0) counterpart, inclusion of the exchange–correlation correction substantially increases the computational cost of the method. SIC(30,10) provides only a modest 20% speedup rela-

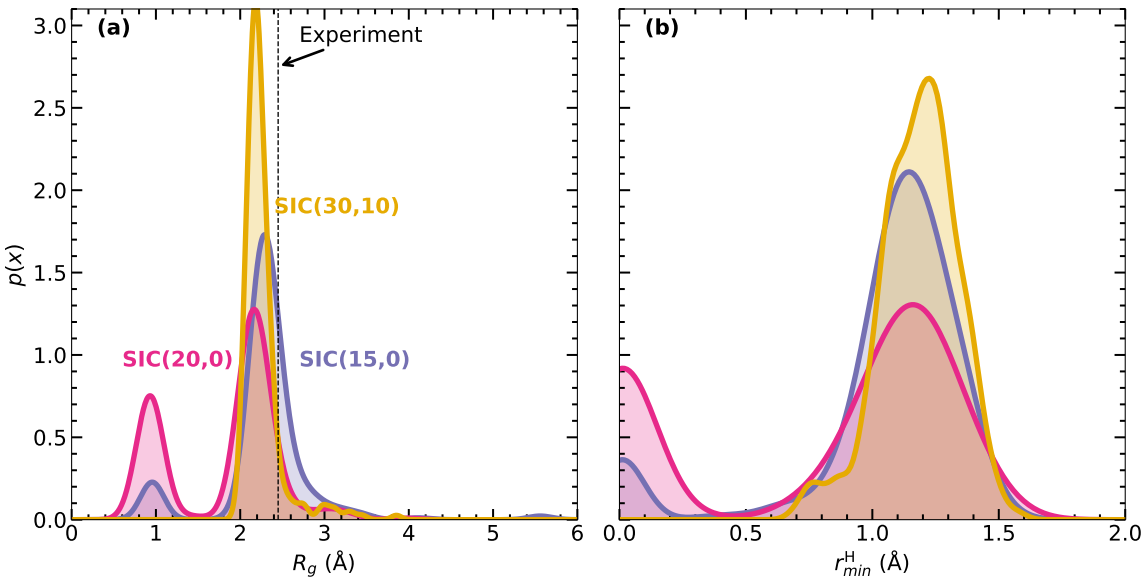

Figure 4: **a.** Probability density of the radius of gyration of the spin density for SIC(15,0)-revPBE-D3 (purple), SIC(20,0)-revPBE-D3 (pink), and SIC(30,10)-revPBE-D3 (yellow). **b.** The corresponding probability density for the distance between the centroid of the spin density and the nearest hydrogen atom. Probability density functions are computed through a Gaussian kernel density estimation.

tive to PBEh(40)-D3, compared to a more than 55% reduction in computational time for SIC(15,0). Memory requirements are slightly reduced, by $\sim$ 12% and 25% for SIC(30,10) and SIC(15,0), respectively. Nevertheless, SIC-GGA functionals are expected to scale more favorably with system size than hybrids due to the absence of the four-center Hartree–Fock integrals.

We also calculate the partial molar volume, V_M, of the hydrated electron within the different descriptions based on the RDFs shown in Fig. 3.[43] We note, however, that these are merely estimates as an accurate determination of V_M requires much larger simulation cells, *e.g.*, $\sim$ 2000 molecules,[43] that are not accessible with DFT-MD. The partial molar volumes obtained with the SIC(15,0) and SIC(20,0) models are slightly reduced relative to the PBEh(40)-D3 result of 7.5 cm^3/mol, which is itself smaller than (but carrying the right sign as) the experimental value of 26 $\pm$ 6 cm^3/mol.[44] The SIC(30,10) description gives a V_M identical to the PBEh(40) result. However, the differences observed between the various density functional approximations are not distinguishable within the statistical errors (even with 120 ps of total simulation time).

Finally, we have also tested an SIC-based approach for the PBE-D3 functional that was recently introduced in the literature for simulating the reactivity of the hydrated electron with per- and polyfluoroalkyl substances.[25] It differs from the orbital-by-orbital SIC approaches considered here in that it makes use of an average-density (AD) SIC, where the self-interaction potentials over the different spin orbitals are averaged to produce a non-local correction applied to all orbitals.[45,46] The technical details and results of an ensemble of hydrated electron trajectories simulated with this AD-SIC-PBE-D3 functional are presented in the SI. Note that we have not attempted to optimize this functional using our spin density

criteria but instead only evaluate its performance to provide insight on the effectiveness of a global SIC correction scheme on a functional similar to revPBE.

As shown in Fig. S6, the corresponding spin densities computed with AD-SIC-PBE-D3 are of similar quality to those obtained with the uncorrected revPBE-D3 functional when evaluated for configurations obtained with PBEh(40)-D3, and the excess electron remains delocalized throughout the simulation cell when it is used to propagate dynamics. We note that this functional was optimized to reproduce the vertical detachment energies of per- and polyfluoroalkyl substances using higher levels of theory,[25] and thus it is perhaps not surprising that it does not perform adequately in this test.

Overall, our results indicate that agreement with reference spin densities is a necessary but insufficient condition for the development of a viable SIC-modified functional for the hydrated electron. Moreover, the analysis of the individual trajectories emphasizes the importance of starting simulations from as many uncorrelated configurations as possible and propagating dynamics for more than a few ps, as unphysical reactivity might otherwise go undetected. These observations underscore the importance of extensive sampling when tuning SIC functionals, as physically unreasonable behaviors that are not pervasive may be fortuitously hidden.

Reduction of Zn(II) with Self-Interaction-Corrected revPBE-D3

A fortuitous, yet important, feature of the PZ–SIC scheme within the ROKS formalism, particularly for simulations of hydrated electron reactions, is that it does not influence the behavior of the system's closed-shell moieties. This property is especially valuable in cases where the inclusion of exact Hartree–Fock exchange can perturb the coordination shell of a closed-shell solute, such as Zn(II), in aqueous solution. In Fig. S8, we show the Zn(II)–O radial distribution functions and coordination number calculated with revPBE-D3, revPBEh(40)-D3, and PBEh(40)-D3 for an aqueous Zn(II) system without the hydrated electron. Clearly, inclusion of Hartree–Fock exchange reduces the coordination number of the ion from six to four and thus makes it is impossible to accurately simulate the reduction of Zn(II) by the hydrated electron in aqueous solution using PBEh(40)-D3.[47,48] It is thus tempting to consider the SIC schemes as a way to address this issue. In fact, while SIC functionals have been used in prior reactivity studies, their ability to accurately describe the hydrated electron has not always been fully validated.[25,26]

To explore the reactivity of the hydrated electron and assess the system-size dependence of the SIC-revPBE-D3 functionals, we doubled the number of water molecules in the simulation cell from 64 to 128 and modeled the reduction of Zn(II) at 25°C and 1.0024 g/cm^3 using the SIC(30,10) functional. The analysis presented in Fig. S7 demonstrates that the observed overlocalization phenomena of the SIC(15,0) functional is not a finite size artifact and further confirms that this functional is unreliable for simulating the hydrated electron.

With regards to reactivity, Bartels *et al.* experimentally determined the corresponding rate constant at zero ionic strength to be $(0.16 \pm 0.01) \times 10^{10}$ M^{-1}s^{-1}.[15] Given that our simulation cell has $[e^-_{aq}] = [\mathrm{Zn(II)}] = 0.432$ M, the probability of a reaction occurring within 5 ps is approximately 3.5×10^{-3}, which corresponds to a reaction in approximately 1 out of every 900 trajectories. In other words, it is vanishingly unlikely to

observe a reactive event using conventional simulation techniques if the functional appropriately describes the hydrated electron and the Zn(II) ion. As shown in Fig. 5a, using the instantaneous distance between the centroid of the spin density and the zinc ion, we do not observe a successful reaction with the SIC(30,10) functional. However, the hydrated electron does react, just not with Zn(II). The presence of the metal ion appears to accelerate the reaction of e^-_{aq} with a water molecule; this can be seen from the three trajectories shown in Fig. 5b where the excess electron localizes on a hydrogen atom, $r^{\mathrm{H}}_{min} \rightarrow 0$. This clearly indicates that this SIC scheme is not reliable for predicting the reactivity of the hydrated electron with Zn(II).

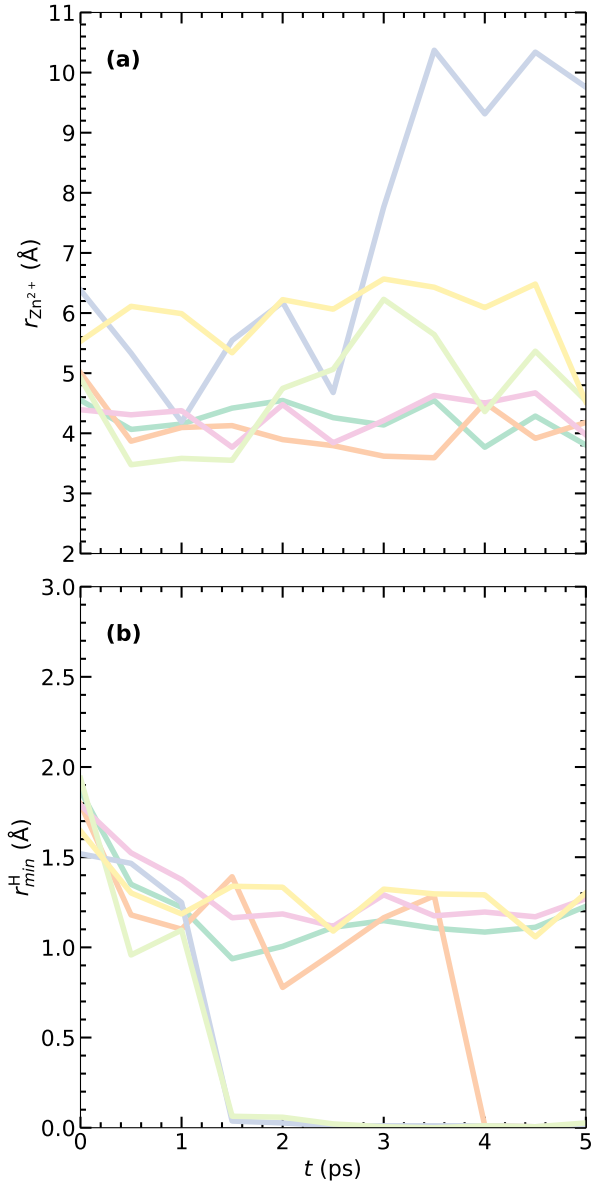

Figure 5: **a.** Distance between the spin density centroid and the position of the Zn(II) ion. **b.** Distance between the centroid of the spin density and the nearest hydrogen atom. Each color corresponds to a unique SIC(30,10) trajectory.

Discussion

Self-Interaction-Error Influence over Localization

It is known from DFT simulations that an excess electron introduced into water with a pre-equilibrated solvent cavity present will localize into the cavity to form a hydrated electron if the chosen functional can describe the species.[23] In the presence of two quasi-degenerate solvent cavities that are sufficiently far apart in space, an excess electron would be expected to localize into whichever cavity is most energetically favorable, rather than delocalize into both. Since this phenomenon can be seen as analogous to the localization of the electron in the $H_2{}^+$ molecule at the dissociation limit, it is sensible to suspect that functionals suffering from self-interaction error will favor delocalization. Thus, the extent to which an excess electron delocalizes across both cavities can be used as a semi-quantitative metric of SIE.

To this end, we prepared water configurations with two nearly identical solvent cavities by simulating 2 Cl^- ions in a 128-water simulation cell of side length 15.81 Å. One classical MD simulation, following the setup described in the Methods section, was used to generate the structures from which 4

independent *ab initio* trajectories were initiated. We used the r^{2}SCAN meta-GGA functional[49] to equilibrate the system at the DFT level; this functional is known to provide a reasonable description of liquid water at room temperature[50,51] and eliminates any bias toward one of the functionals to be evaluated. A total of 8 configurations were extracted every 25 fs from the last 200 fs of the DFT trajectories, and both chlorine atoms are removed before a single excess electron is added to the system. The localization of the excess electron was determined through an analysis of the spin density, which was obtained from single-point calculations without structural relaxation using HF, PBEh(40), revPBE, and SIC-revPBE. Specifically, we integrated the numerical spin density within 3 Å radius spheres centered on the coordinates of the chlorine atoms, which were more than 6 Å apart.

$$m(\mathbf{r}_j) = \int_{|\mathbf{r}-\mathbf{r}_j|} d^3r \; m(\mathbf{r}), \qquad (3)$$

where $\mathbf{r}_j$ the position of cavity j with $j = 1$ or 2.

The results are presented in Fig. 6 and show that HF, a level of theory free of one-electron SIE by definition, localizes the spin density preferentially into a single cavity, as fully delocalized states with $m(\mathbf{r}_1) = m(\mathbf{r}_2)$ are absent from the distribution. PBEh(40), a hybrid functional that includes 40% HF exchange, tends to favor localization into a single cavity, although it does occasionally predict structures with the electron delocalized across both cavities. On the other hand, revPBE exclusively delocalizes the excess electron into both cavities, unless a self-interaction correction functional is added to it, as exemplified by SIC(30,10). Nevertheless, SIC(30,10) does not completely eliminate the self-interaction error inherited from the parent GGA and notably underperforms relative to PBEh(40). We suspect that SIC(30,10) is inferior to PBEh(40) because the former only treats the SIE affecting the singly occupied molecular orbital.

The effect of systemically varying the self-Coulomb correction, $E_H[m]$, to revPBE is presented in Fig. 6b. Generally, increasing c_H decreases the population of electrons fully delocalized between the cavities, but the effects are modest. Furthermore, the data presented in the Results section indicate that a better localized spin density for static configurations does not guarantee a proper treatment of the energetic barriers encountered in dynamics. We can conclude that $E_H[m]$ successfully removes the self-Coulomb interaction systematically but influences energetic barriers non-intuitively. Inclusion of only the self-exchange-correlation correction, $E_{XC}[m, 0]$, in the SIC(0,10) model worsens the delocalization of the excess electron with respect to revPBE, but the same addition to SIC(30,0) to produce SIC(30,10) improves the description of the localization in Fig. 6 and predicts stable hydrated electron dynamics as shown in Fig. 2.

The data presented in the Results section illustrate that it is rather challenging to systematically improve an SIC functional for the hydrated electron under periodic boundary conditions, as structural metrics do not provide insight into the energetic barriers between the different states populated by the excess electron and it is difficult to compute accurate vertical detachment energies to probe the stability of these structures. One alternative is to examine the thermalization of an excess electron injected into neat water in the absence of pre-equilibrated solvent cavities, as we now discuss.

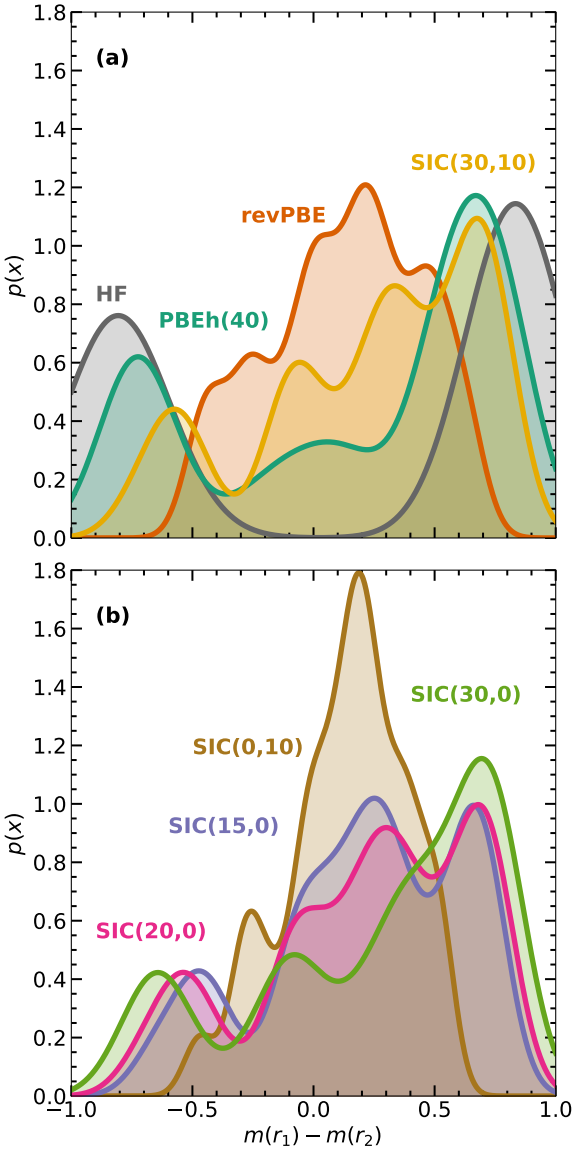

Figure 6: Difference in the amount of excess electron confined within 3 Å spheres centered on positions $\mathbf{r}_1$ and $\mathbf{r}_2$, calculated by the integrating the spin density obtained using **a.** HF (gray), PBEh(40)-D3 (cyan), SIC(30,10)-revPBE-D3 (yellow), revPBE-D3 (orange), **b.** SIC(15,0)-revPBE-D3 (purple), SIC(20,0)-revPBE-D3 (pink), SIC(30,0)-revPBE-D3 (green), and SIC(0,10)-revPBE-D3 (brown).

Localization Barriers with Self-Interaction-Corrected revPBE-D3

Experiment and simulation have established that an excess electron will localize and thermalize into the hydrated electron within hundreds of fs when injected into neat water at room temperature.[52–55] This behavior should be generally reproduced by a DFT functional that properly treats the electronic levels of an excess electron in water. PBEh(40) is known to accurately describe injection dynamics,[30] so we simulate the localization dynamics of an excess electron injected into neat water using SIC(30,0), SIC(30,5), SIC(30,10), and SIC(30,20) to gain qualitative insight into the energetics of the delocalized and localized states of the hydrated electron at the SIC-DFT level of theory. By holding the Hartree contribution to the SIC constant while varying the XC contribution, one can also examine the influence of the latter in the "absence" of self-Coulomb interaction.

We used a cubic simulation cell of side length 9.86 Å with 32 SPC/Fw waters[39] in classical MD simulations to create an ensemble of initial configurations for our SIC-DFT-based injection dynamics trajectories. Eight uncorrelated configurations were extracted from the equilibrated portion of the classical MD trajectory and used to initiate dynamics with an excess electron added to the system. Four ps of simulation time were collected for SIC(30,0), SIC(30,5), SIC(30,10), and SIC(30,20) using the same simulation protocols employed for our equilibrium hydrated electron simulations. We also include data for PBEh(40) to demonstrate that it localizes an excess electron in a sub-picosecond timescale under these conditions.

We find that SIC(30,10) successfully localizes an excess electron, as shown in Figs. 7 and S9, but at a timescale ($\tau > 1$ ps) that is slow compared to experiment; in 3 out of 8 trajectories the excess electron remains delocalized for the full 4 ps of the trajectory. This indicates that the functional does place the hydrated electron at a lower energy rel-

ative than the delocalized state, but that it does not quantitatively capture the energy difference and/or the energetic barrier between these two states.

The exclusion of $E_{XC}[m,0]$ further worsens the description of excess electron localization, as demonstrated by the failure of SIC(30,0) to form a stable hydrated electron within 4 ps in any of the eight trajectories, illustrated in Fig. 7a by the compact radius of gyration of the spin density. As was seen with our pre-equilibrated cavity simulations, rather than forming a delocalized or localized hydrated electron, SIC(30,0) instead favors reaction with water to form OH^- and H·, but we also observed it form an OH·, OH^-, and an H_2 molecule in 1 trajectory. The reactivity can be seen by the distance between the centroid of the spin density and its nearest H atom, as shown in Fig. 7b. When these results are rationalized with the insight provided by Figs. 6 and 2, we can reasonably speculate that it is not possible to correct SIE using PZ-SIC exclusively on the SOMO.

Increasing the exchange-correlation correction to the SIC(30,20) model, results in complete failure to localize the excess electron in all eight trajectories, as shown in Fig. 7a. No reactions were observed either, as shown in Fig. 7b. We can conclude that $E_{XC}[m,0]$ lowers the energy of the delocalized state relative to the localized hydrated electron, which is not in accord with experiment. Similarly, decreasing c_{XC} from 0.10 to 0.05 to construct SIC(30,5) reduces the number of reactions with water from 8 to 1 relative to SIC(30,0), yields stable hydrated electrons, but still does not predict a localization timescale in agreement with either PBEh(40) or experiment.

As shown in Fig. S10, the SIC(30,20)-PBE functional used by Marsalek *et al.*,[34] which has previously been successfully used to study the reaction of the hydrated electron with a hydronium ion in water clusters (non-periodic conditions), also failed to localize the excess electron when injected into neat water. Because SIC(30,20)-PBE was tuned to replicate the energies of gas phase clusters evaluated at the RI-UMP2/aug-cc-pVDZ level of theory, our results suggest that the energetic barrier between the delocalized and localized states of the hydrated electron are not treated accurately in the bulk liquid phase by this functional.

A similar approach, using the SIC(30,20) correction on the SOMO and a semi-empirical treatment of dispersion, but with the BLYP functional was used by Uhlig et al. in quantum mechanics/molecular mechanics (QM/MM) simulations of an excess electron in neat water.[56] Interestingly, the c_{H} and c_{XC} scaling parameters for the SIC scheme used were taken from the SIC(30,20)-PBE study of water clusters given in Ref. 34, without further optimization.[57] Using 32 quantum mechanical waters surrounded by 992 classical ones, they found a radius of gyration of $\sim$ 2.8 Å and a vertical detachment energy of $\sim$ 3 eV, larger and smaller, respectively, than experimental measurements.[56] It is unclear if the successful localization of the electron with this approach, in contrast to the failure we observe for the SIC(30,20)-PBE model, is due to the difference in functional or the QM/MM description.

We note that PBEh(40) treats SIE by adding a fixed amount (x) of exact HF exchange, but it also removes a complementary amount, $1-x$, of approximate PBE exchange while keeping PBE correlation constant. PZ-SIC, on the other hand, removes SIE by subtracting $E_H[m]$ and $E_{XC}[m,0]$. Because PZ-SIC scheme introduces the complexity of altering the correlation functional as well, we can only point out that its inclusion seems to ameliorate the over localization tendencies systematically introduced

by $E_H[m]$ but does not improve the energetic barriers between the states of the excess electron in a manner that yields predictions in satisfactory agreement with experiment. Thus, these results suggest that SIC functionals could benefit from an optimization protocol that targets the electronic levels of an excess electron in the aqueous solution of interest, as established for PBEh(40) by Ambrosio *et al.*[22]

Conclusions

We have systematically assessed the performance of two distinct self-interaction correction schemes in describing the chemistry of an excess electron in water. We found that the Perdew–Zunger SIC approximation could be used to develop ostensibly promising DFT descriptions of the hydrated electron by tuning the SIC parameters for revPBE to reproduce the spin density predicted by PBEh(40). On the other hand, an average-density SIC functional based on PBE that has been previously used in the literature does not remedy the overdelocalization problem in neat water inherited from its parent GGA functional. It remains to be seen if the AD-SIC functional can predict stable hydrated electron dynamics after it is tuned to reproduce the spin densities from PBEh(40) hydrated electron configurations.

While some functionals based on the PZ-SIC approach successfully reproduce the hydrated electron behavior when applied to static configurations extracted from PBEh(40)-based simulations, they do not provide a reliable basis for DFT-MD simulations themselves. Specifically, we found that SIC-GGA functionals that include only the Hartree (E_H) correction either fail to suppress the delocalization of the excess electron originating from the self-interaction error or instead drive an unphysical over-

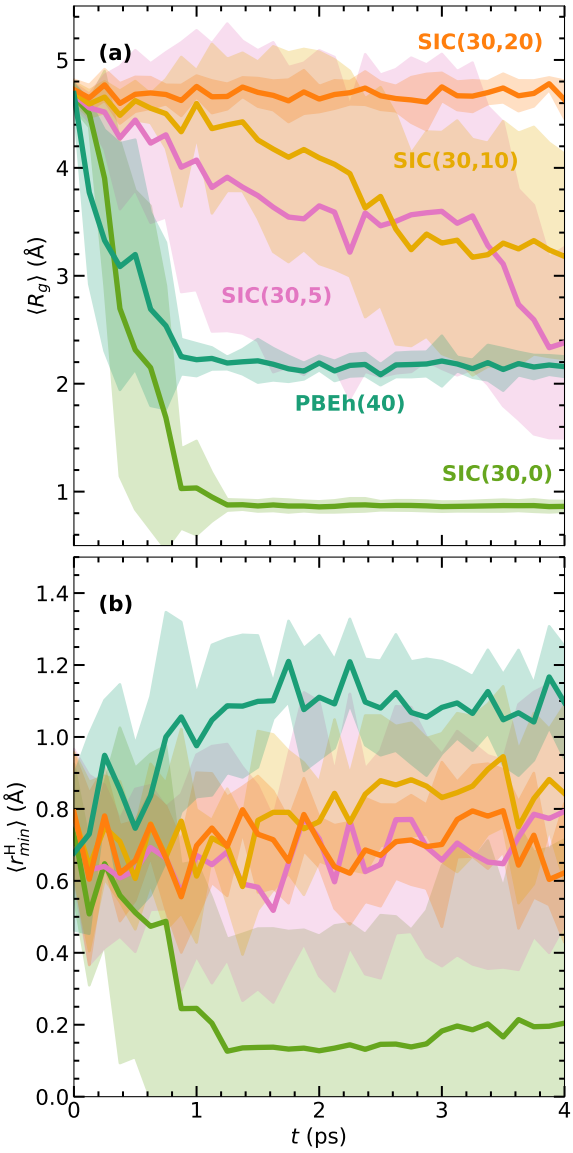

Figure 7: **a.** Average radius of gyration of the spin density and **b.** its centroid's minimal distance to a hydrogen atom for an excess electron injected into neat SPC/Fw water configurations. DFT dynamics were propagated using SIC(30,0)-revPBE-D3 (green), SIC(30,5)-revPBE-D3 (purple), SIC(30,10)-revPBE-D3 (yellow), SIC(30,20)-revPBE-D3 (orange) and PBEh(40) (cyan). Shaded regions correspond to one standard deviation.

localization of the excess electron onto a hydrogen atom, *i.e.*, reaction with a water

molecule.

Furthermore, great caution must be exercised when using such correction schemes to simulate the hydrated electron. That is, in some cases we found multiple trajectories for a given SIC-GGA functional that provide a reasonable description of the hydrated electron, but this is not the case for all the trajectories. Thus, in a limited number of short trajectories it may erroneously appear that a given functional may successfully represent the hydrated electron behavior because insufficient sampling is masking a failure to provide a fully robust description of the underlying physics.

We successfully optimized an SIC-revPBE-D3 functional to accurately reproduce the spin density and average dynamical properties of the PBEh(40) hydrated electron by inclusion of an exchange-correlation correction. However, when we applied it in simulations of the hydrated electron in the presence of Zn(II), it predicted significant reactivity with water molecules in contradiction to experimental characterizations.[15] This behavior demonstrates that even SIC-based descriptions that adequately describe the hydrated electron in neat water, including in reasonably sampled DFT-MD simulations, must still be fully validated for use in describing solutions and reactivity.

Supporting Information

The Supporting Information is provided as a PDF file and contains the following data: Convergence thresholds for DFT-MD simulations, self-interaction-corrected spin densities, SIC-revPBE MD spin densities, data from DFT-MD simulations, average-density self-interaction-corrected PBE-D3, system-size effects on SIC(15,0) DFT-MD, Zn(II) coordination number in liquid water

Notes

The authors declare no competing financial interests.

Acknowledgments

This work was funded by the Division of Chemical Sciences, Geosciences, and Biosciences, Office of Basic Energy Sciences of the U.S. Department of Energy, through grant no. DE-SC0021114 (W.H.T.). D.M.B. is supported by the U.S. Department of Energy Office of Science, Office of Basic Energy Sciences under Award Number DE-FC02-04ER1553. The calculations were performed at the University of Kansas Center for Research Computing (CRC), including the BigJay cluster resource funded through NSF Grant MRI-2117449.

References

(1) Hart, E. J. *Solvated Electron*; ACS Publications, 1965; Vol. 50.

(2) Hart, E. J. The significance of the hydrated electron in radiation chemistry. *Health Physics* **1966**, *12*, 641–651.

(3) Walker, D. C. The hydrated electron. *Q. Rev., Chem. Soc.* **1967**, *21*, 79–108.

(4) Daily, R.; Minakata, D. Reactivities of hydrated electrons with organic compounds in aqueous-phase advanced reduction processes. *Environ. Sci.: Water Res. Technol.* **2022**, *8*, 543–574.

(5) Maza, W. A.; Breslin, V. M.; Owrutsky, J. C. Early steps in the advanced reduction process of the hydrated electron: lessons learned from transient spectroscopy. *Curr. Opin. Chem. Eng.* **2024**, *44*, 101015.

(6) Bartels, D. M.; Thompson, W. H. Reactivity of the Hydrated Electron. *Annu. Rev. Phys. Chem.* **2025**, *77*.

(7) Turi, L.; Rossky, P. J. Theoretical studies of spectroscopy and dynamics of hydrated electrons. *Chem. Rev.* **2012**, *112*, 5641–5674.

(8) Herbert, J. M. Structure of the aqueous electron. *Phys. Chem. Chem. Phys.* **2019**, *21*, 20538–20565.

(9) Gordon, S.; Hart, E. J.; Matheson, M. S.; Rabani, J.; Thomas, J. Reaction constants of the hydrated electron. *J. Am. Chem. Soc.* **1963**, *85*, 1375–1377.

(10) Hart, E. J.; Gordon, S.; Thomas, J. Rate constants of hydrated electron reactions with organic compounds[1]. *J. Phys. Chem.* **1964**, *68*, 1271–1274.

(11) Hart, E. J.; Thomas, J.; Gordon, S. A review of the radiation chemistry of single-carbon compounds and some reactions of the hydrated electron in aqueous solution. *Radiat. Res. Suppl.* **1964**, *4*, 74–88.

(12) Hart, E. J.; Fielden, E. M.; Anbar, M. Reactions of carbonylic compounds with hydrated electrons. *J. Phys. Chem.* **1967**, *71*, 3993–3998.

(13) Anbar, M. *Adv. Phys. Org. Chem.*; Elsevier, 1969; Vol. 7; pp 115–151.

(14) Buxton, G. V.; Greenstock, C. L.; Phillips Helman, W.; Ross, A. B. Critical review of rate constants for reactions of hydrated electrons. *J. Phys. Chem. Ref. Data* **1988**, *17*.

(15) Kanjana, K.; Courtin, B.; MacConnell, A.; Bartels, D. M. Reactions of hexa-aquo transition metal ions with the hydrated electron up to 300°C. *J. Phys. Chem. A* **2015**, *119*, 11094–11104.

(16) Lisovskaya, A.; Bartels, D. M. Reduction of CO_2 by hydrated electrons in high temperature water. *Radiat. Phys. Chem.* **2019**, *158*, 61–63.

(17) Fennell, B. D.; Fowler, D.; Mezyk, S. P.; McKay, G. Reactivity of dissolved organic matter with the hydrated electron: Implications for treatment of chemical contaminants in water with advanced reduction processes. *Environ. Sci. Technol.* **2023**, *57*, 7634–7643.

(18) Herbert, J. M.; Jacobson, L. D. Structure of the aqueous electron: Assessment of one-electron pseudopotential models in comparison to experimental data and time-dependent density functional theory. *J. Phys. Chem. A* **2011**, *115*, 14470–14483.

(19) Neupane, P.; Bartels, D. M.; Thompson, W. H. Empirically optimized one-electron pseudopotential for the hydrated electron: A proof-of-concept study. *J. Phys. Chem. B* **2023**, *127*, 7361–7371.

(20) Tapavicza, E.; Meyer, A. M.; Furche, F. Unravelling the details of vitamin D photosynthesis by non-adiabatic molecular dynamics simulations. *Phys. Chem. Chem. Phys.* **2011**, *13*, 20986–20998.

(21) Marsalek, O.; Uhlig, F.; Vandevondele, J.; Jungwirth, P. Structure, dynamics, and reactivity of hydrated electrons by ab initio molecular dynamics. *Acc. Chem. Res.* **2012**, *45*, 23–32.

(22) Ambrosio, F.; Miceli, G.; Pasquarello, A. Electronic levels of excess electrons in liquid water. *J. Phys. Chem. Lett.* **2017**, *8*, 2055–2059.

(23) Borrelli, W. R.; Liu, X.; Schwartz, B. J. How the choice of exchange–correlation functional affects DFT-based simulations of the hydrated electron. *J. Chem. Phys.* **2025**, *162*.

(24) Renault, J. P.; Vuilleumier, R.; Pommeret, S. Hydrated electron production by reaction of hydrogen atoms with hydroxide ions: A first-principles molecular dynamics study. *J. Phys. Chem. A* **2008**, *112*, 7027–7034.

(25) Biswas, S.; Yamijala, S. S.; Wong, B. M. Degradation of per- and polyfluoroalkyl substances with hydrated electrons: a new mechanism from first-principles calculations. *Environ. Sci. Technol.* **2022**, *56*, 8167–8175.

(26) Renault, J. P.; Pommeret, S. Seeing the solvated electron in action: First-principles molecular dynamics of NO^{3-} and N_2O reduction. *Radiat. Phys. Chem.* **2022**, *190*, 109810.

(27) Neupane, P.; Bartels, D. M.; Thompson, W. H. Exploring the unusual reactivity of the hydrated electron with CO_2. *J. Phys. Chem. B* **2024**, *128*, 567–575.

(28) Narvaez, W. A.; Neupane, P.; Bartels, D. M.; Thompson, W. H. Ab Initio Molecular Dynamics Study of the Reduction of Acetone by the Hydrated Electron. *J. Phys. Chem. B* **2025**, *129*, 8201–8209.

(29) Borrelli, W. R.; Liu, X.; Schwartz, B. J. Evaluating the chemical reactivity of DFT-simulated liquid water with hydrated electrons via the dual descriptor. *J. Chem. Theory Comput.* **2024**, *20*, 9571–9579.

(30) Pizzochero, M.; Ambrosio, F.; Pasquarello, A. Picture of the wet electron: a localized transient state in liquid water. *Chem. Sci.* **2019**, *10*, 7442–7448.

(31) Perdew, J. P.; Zunger, A. Self-interaction correction to density-functional approximations for many-electron systems. *Phys. Rev. B* **1981**, *23*, 5048.

(32) d'Avezac, M.; Calandra, M.; Mauri, F. Density functional theory description of hole-trapping in SiO_2: A self-interaction-corrected approach. *Phys. Rev. B* **2005**, *71*, 205210.

(33) VandeVondele, J.; Sprik, M. A molecular dynamics study of the hydroxyl radical in solution applying self-interaction-corrected density functional methods. *Phys. Chem. Chem. Phys.* **2005**, *7*, 1363–1367.

(34) Marsalek, O.; Frigato, T.; VandeVondele, J.; Bradforth, S. E.; Schmidt, B.; Schütte, C.; Jungwirth, P. Hydrogen forms in water by proton transfer to a distorted electron. *J. Phys. Chem. B* **2010**, *114*, 915–920.

(35) Pestana, L. R.; Mardirossian, N.; Head-Gordon, M.; Head-Gordon, T. Ab initio molecular dynamics simulations of liquid water using high quality meta-GGA functionals. *Chem. Sci.* **2017**, *8*, 3554–3565.

(36) Lin, I.-C.; Seitsonen, A. P.; Tavernelli, I.; Rothlisberger, U. Structure and Dynamics of Liquid Water from ab Initio Molecular Dynamics Comparison of BLYP, PBE, and revPBE Density Functionals with and without van der Waals Corrections. *J. Chem. Theory Comput.* **2012**, *8*, 3902–3910.

(37) Thompson, A. P.; Aktulga, H. M.; Berger, R.; Bolintineanu, D. S.; Brown, W. M.; Crozier, P. S.; in 't Veld, P. J.; Kohlmeyer, A.; Moore, S. G.; Nguyen, T. D. et al. LAMMPS-a flexible simulation tool for particle-based materials modeling at the atomic, meso, and continuum scales. *Comput. Phys. Commun.* **2022**, *271*, 108171.

(38) Kühne, T. D.; Iannuzzi, M.; Del Ben, M.; Rybkin, V. V.; Seewald, P.; Stein, F.; Laino, T.; Khaliullin, R. Z.; Schütt, O.; Schiffmann, F. et al. CP2K: An electronic structure and molecular dynamics software package-Quickstep: Efficient and accurate electronic structure calculations. *J. Chem. Phys.* **2020**, *152*.

(39) Wu, Y.; Tepper, H. L.; Voth, G. A. Flexible simple point-charge water model with improved liquid-state properties. *J. Chem. Phys.* **2006**, *124*, 024503.

(40) Grimme, S.; Antony, J.; Ehrlich, S.; Krieg, H. A consistent and accurate ab initio parametrization of density functional dispersion correction (DFT-D) for the 94 elements H-Pu. *J. Chem. Phys.* **2010**, *132*.

(41) Guidon, M.; Hutter, J.; VandeVondele, J. Auxiliary density matrix methods for Hartree- Fock exchange calculations. *J. Chem. Theory Comput.* **2010**, *6*, 2348–2364.

(42) Bartels, D. M. Moment analysis of hydrated electron cluster spectra: Surface or internal states? *J. Chem. Phys.* **2001**, *115*, 4404–4405.

(43) Neupane, P.; Bartels, D. M.; Thompson, W. H. Relation between the hydrated electron solvation structure and its partial molar volume. *J. Phys. Chem. B* **2023**, *127*, 5941–5947.

(44) Janik, I.; Lisovskaya, A.; Bartels, D. M. Partial molar volume of the hydrated electron. *J. Phys. Chem. Lett.* **2019**, *10*, 2220–2226.

(45) Legrand, C.; Suraud, E.; Reinhard, P. Comparison of self-interaction-corrections for metalclusters. *J. Phys. B: At. Mol. Opt. Phys.* **2002**, *35*, 1115.

(46) Ciofini, I.; Chermette, H.; Adamo, C. A mean-field self-interaction correction in density functional theory: implementation and validation for molecules. *Chem. Phys. Lett.* **2003**, *380*, 12–20.

(47) Ducher, M.; Pietrucci, F.; Balan, E.; Ferlat, G.; Paulatto, L.; Blanchard, M. van der Waals contribution to the relative stability of aqueous Zn(2+) coordination states. *J. Chem. Theory Comput.* **2017**, *13*, 3340–3347.

(48) Malinowski, A.; Śmiechowski, M. Solvent exchange around aqueous Zn(II) from ab initio molecular dynamics simulations. *Liquids* **2022**, *2*, 243–257.

(49) Furness, J. W.; Kaplan, A. D.; Ning, J.; Perdew, J. P.; Sun, J. Accurate and numerically efficient r2SCAN

meta-generalized gradient approximation. *J. Phys. Chem. Lett* **2020**, *11*, 8208–8215.

(50) Chen, M.; Ko, H.-Y.; Remsing, R. C.; Calegari Andrade, M. F.; Santra, B.; Sun, Z.; Selloni, A.; Car, R.; Klein, M. L.; Perdew, J. P. et al. Ab initio theory and modeling of water. *Proc. Natl. Acad. Sci. U. S. A.* **2017**, *114*, 10846–10851.

(51) Wang, C.; Tian, W.; Zhou, K. Ab initio simulation of liquid water without artificial high temperature. *J. Chem. Theory Comput.* **2024**, *20*, 8202–8213.

(52) Migus, A.; Gauduel, Y.; Martin, J.; Antonetti, A. Excess electrons in liquid water: first evidence of a prehydrated state with femtosecond lifetime. *Phys. Rev. Lett.* **1987**, *58*, 1559.

(53) Long, F. H.; Lu, H.; Eisenthal, K. B. Femtosecond studies of the presolvated electron: an excited state of the solvated electron? *Phys. Rev. Lett.* **1990**, *64*, 1469.

(54) Narvaez, W. A.; Wu, E. C.; Park, S. J.; Gomez, M.; Schwartz, B. J. Trap-seeking or trap-digging? Photoinjection of hydrated electrons into aqueous NaCl solutions. *J. Phys. Chem. Lett.* **2022**, *13*, 8653–8659.

(55) Carter-Fenk, K.; Johnson, B. A.; Herbert, J. M.; Schenter, G. K.; Mundy, C. J. Birth of the hydrated electron via charge-transfer-to-solvent excitation of aqueous iodide. *J. Phys. Chem. Lett.* **2023**, *14*, 870–878.

(56) Uhlig, F.; Marsalek, O.; Jungwirth, P. Unraveling the complex nature of the hydrated electron. *J. Phys. Chem. Lett.* **2012**, *3*, 3071–3075.

(57) Uhlig, F.; Marsalek, O.; Jungwirth, P. From a localized H_3O radical to a delocalized $H_3O^+ \cdots e^-$ solvent-separated pair by sequential hydration. *PCCP* **2011**, *13*, 14003–14009.

TOC Graphic